A QUANTITATIVE ANALYSIS OF THE VOLTAGE-CURRENT RELATIONSHIPS OF FIXED CHARGE MEMBRANES AND THE ASSOCIATED PROPERTY OF "PUNCH-THROUGH"

H. G. L. COSTER

From the Plant Physiology Unit, C.S.I.R.O. Division of Food Preservation and School of Biological Sciences, University of Sydney, Sydney, New South Wales, Australia

ABSTRACT A theoretical analysis of the voltage-current relationship is carried out in a membrane consisting of two fixed charge regions, of opposite sign, in contact. This is achieved by applying the diffusion equations to this system in conjunction with the Poisson-Boltzmann equation. The latter has been successfully applied by Mauro to determine the profiles of the electrostatic potential in his treatment of the capacitative property of such a system. It is shown that the system displays the property of rectification and is very similar in many respects to a solid state P-N junction diode. It is also shown that for the case of reverse bias, an electrical breakdown phenomena can occur. This is referred to as the "punch-through" effect. "Punch-through" was observed in experiments on the electrical characteristics of the membranes of *Chara australis* and *Nitella* sp. The experimental results are discussed in relation to the theoretical analysis.

INTRODUCTION

The electrical properties of a thin membrane separating two ionic solutions has been studied fairly intensively. Among these properties studied for the membranes of biological systems have been the resting potential, action potentials, the voltage-current characteristics, and the membrane capacitance.

It has usually been assumed that the observed capacitance is simply due to the separation of two conductors (*i.e.*, the ionic solutions) by insulating membranes. Hence, by assuming certain values for the dielectric constant of the membrane, the observed capacitance of about 1 $\mu f/cm^2$ could be explained. However, Mauro (1962) has recently shown that the transition regions of a double lattice in which one side has fixed positive charges and the other fixed negative charges, will display the conservative property of capacitance. He showed that the capacitance in this case is equal to that of a parallel plate capacitor in which the plates are separated by a distance equal to the thickness of the "depletion" layer at the transition.

A comprehensive treatment of some of the electrical properties of single fixed charge membranes, including rectification, has been given by Meyer, Sievers, and Teorell (see Teorell 1953).

The voltage-current characteristics of the plasmalemma in *Chara* cells are adequately described by the Goldman model (Goldman, 1943), but this is not generally true of other membranes.

On plotting V-I characteristics (obtained by a current scanning technique) of the membranes of *Chara australis,* the author observed that for sufficiently large negative (*i.e.,* hyperpolarizing) potentials, the current suddenly increases very rapidly. This is very similar to a dielectric breakdown. The breakdown, however, is not destructive, as the whole scan can be repeated over and over again to give the same V-I curves, and the breakdown occurs each time at the same potential. It is fairly sharp and is very similar to a "punch-through" observed in solid state P-N junction diodes. The same effect was observed in the V-I characteristics of *Nitella* sp.

In view of Mauro's successful application of the Poisson-Boltzmann equation to fixed charge membranes in relation to the property of capacitance, and in view of the observed breakdown effect, a theoretical analysis of the voltage-current relationship of fixed charge membranes has been made, in an attempt to explain the observed V-I characteristics, including the breakdown phenomena.

THEORY

The fixed charge membranes to be considered in this paper are those which for simplicity have a homogeneous distribution of fixed charges. These may be due to fixed ionized groups attached to a lattice network. It will be assumed that mobile ions are free to move in a dielectric solution which permeates the lattice network. It is also assumed that the fixed charges can be regarded as point charges, and that the lattice network merely serves to fix the charges and does not contribute otherwise to the electrical properties of the membrane. Both the fixed and the mobile ions will be considered as singly charged.

Since in most biological systems the membrane separates a solution of ions inside the cell from an ionic solution of different concentration outside the cell, it is this type of system that will be considered. Such a system also displays a membrane potential, V_m.

Throughout this paper the rationalized M.K.S. system of units will be used.

In order to determine the profiles of mobile ion concentration and electrostatic potential in the fixed charge lattice it will be assumed that all the mobile ions satisfy the Maxwell-Boltzmann distribution. Consider, for example, the solution lattice interface region depicted in Fig. 1. For regions where the electric potential is $\Psi(x)$:

$$P(x) = P_0 e^{-q[\Psi(x)-\Psi(-\infty)]/KT}$$

and

$$N(x) = N_0 e^{+q[\Psi(x)-\Psi(-\infty)]/KT} \qquad (1)$$

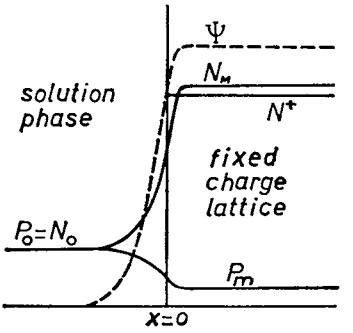

FIGURE 1 A single fixed charge lattice which extends from $x = 0$ to the right and contains fixed positive charges. The profiles for the electrostatic potential, ψ, and the concentration of mobile ions are shown qualitatively. $N_o = P_o$ is the concentration of these ions in the solution phase at large distances from the fixed charge lattice (*i.e.*, where $\psi = 0$).

where P_o and N_o are concentrations of $+ve$ and $-ve$ mobile ions respectively in the region where $\Psi = \Psi(-\infty)$; $P(x)$ and $N(x)$ are the concentrations of these ions at the point x; K = Boltzmann's constant; T = temperature in degrees absolute; q is the unit of electrical charge on the ions and the fixed charges, *i.e.*, $q = |e|$.

The next assumption is that the electrostatic potential, Ψ, satisfies Poisson's equation.

$$\frac{d^2\Psi(x)}{dx^2} = \frac{-p(x)}{\epsilon} \tag{2}$$

where p is the charge density in coul/m^3, and ε is the electric permittivity, $\varepsilon = \varepsilon_R \varepsilon_o$, ε_R is the relative electric permittivity, and ε_o is the permittivity of free space.

If the density of positive and negative fixed charges is N^+ and N^- respectively, then, in a region where there are only positive fixed charges,

$$p(x) = q[P_0 e^{-q(\Psi(x)-\Psi(-\infty))/KT} - N_0 e^{+q(\Psi(x)-\Psi(-\infty))/KT}] + qN^+ \tag{3}$$

Now assuming that $N_o = P_o$ in the solution phase at a large distance from the lattice boundary (this is demanded by electrical neutrality), and also that $\Psi(-\infty) = 0$, one can, using Poisson's equation, write:

$$\frac{d^2\Psi(x)}{dx^2} = \frac{2qN_0}{\epsilon}\left[\sinh\frac{q\Psi(x)}{KT} - \frac{N^+}{2N_0}\right] \tag{4}$$

By solving this equation the profiles of $\Psi(x)$ and hence also $P(x)$ and $N(x)$ can be plotted as a function of x, for a given value of N^+. Mauro (1962) has shown that the potential rises very rapidly inside the lattice and falls off much more slowly in the solution phase. The profiles are shown qualitatively in Fig. 1.

When two lattices of opposite fixed charge are brought in close proximity in an ionic solution the space charge regions in the solution phase at the boundary of

each lattice will interact, and with reducing distance of separation the space charge regions will be forced further into the lattice. In the limit, when the distance of separation is zero, the space charge will reside completely in the opposite fixed charge lattices.[1] This in solid state physics nomenclature is known as an "abrupt junction." The profiles of P and N for such an "abrupt junction" are shown in Fig. 2.

The fixed charge lattice to be considered, depicted in Fig. 2, extends from $x = -W_o$ to $x = W_o$ (*i.e.*, a total width of 2 W_o). The region between $x = -W_o$

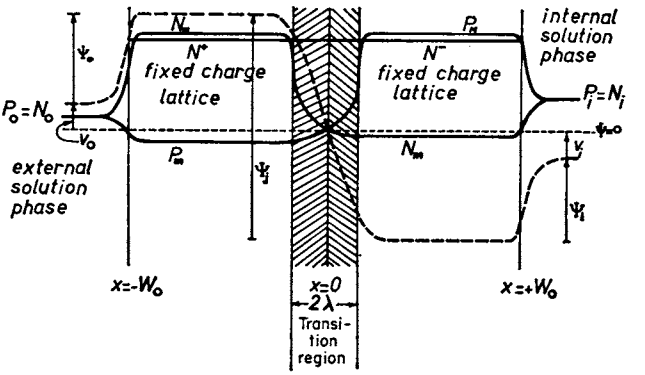

FIGURE 2 Double lattice fixed charge membrane in which the region between $x = -W_o$ and $x = 0$ has fixed positive charges and is in contact with the region between $x = 0$ and $x = +W_o$ which contains fixed negative charges. The profiles for the mobile ion concentrations and the electrostatic potential, ψ, are shown qualitatively. $\psi = 0$ is taken arbitrarily at $x = 0$ as shown. Note that the usual membrane potential, V_m, in this case equals $V_o + V_i$. The profiles for the concentration of mobile ions do not necessarily cross exactly at point $\psi = 0$.

and $x = 0$ has positive fixed charges, while that between $x = 0$ and $x = W_o$ has negative fixed charges. The ionic solutions extend to the left of $x = -W_o$ and to the right of $x = W_o$ for an infinite length.

In the N^- region there will be a predominance of positive mobile ions, P_M, and a minority of negative mobile ions, N_m, while in the N^+ region there will be a predominance of negative mobile ions, denoted N_M, and a minority of positive mobile ions, P_m.

As pointed out before, the space charge will reside exclusively in the fixed charge regions for an abrupt junction, so that as long as N^+ and N^- are large compared to N_o and P_o, the fixed charges in the neighborhood of the junction at $x = o$ will be almost completely uncompensated by the mobile ions. Hence an approximation to the space charge density in this transition region is given by the density of fixed charges in the lattice. Fig. 3 is an idealized profile of the mobile ion concentration.

[1] For a discussion of space charge regions in these transition regions the reader is referred to Mauro (1962); Kittel (1957); Le Can *et al.* (1962).

In accordance with solid state physics terminology, the transition region is referred to as the depletion layer. The depletion layer in Fig. 3 extends from $x = -\lambda$ to $x = +\lambda$.

Using the Maxwell-Boltzmann distribution law, and with reference to Fig. 3, the values of P_M, N_M, *etc.*, can be determined, in terms of P_i, N_o, *etc.*

Thus,

$$P_M = P_i e^{+q\Psi_i/KT} \quad \text{and} \quad N_M = N_0 e^{+q\Psi_o/KT} \tag{5}$$

$$N_m = N_i e^{-q\Psi_i/KT} \quad \text{and} \quad P_m = P_0 e^{-q\Psi_o/KT} \tag{6}$$

When a bias voltage, V, is applied, the concentration of the minority mobile ion concentrations N_m and P_m at the depletion layer boundary at $x = \pm\lambda$, denoted N_j

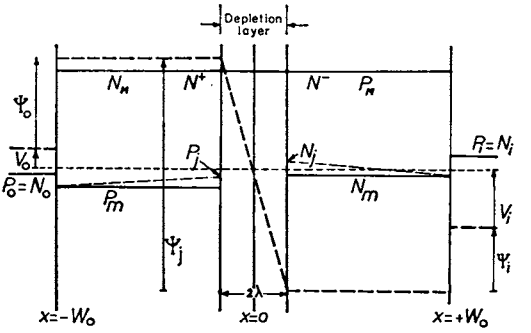

FIGURE 3 Idealized profiles for the concentration of the mobile ions in an "abrupt" junction. The values of the concentration of the minority positive ions in the N^+ region and the minority negative ions in the N^- region, at the depletion layer boundary, are denoted by P_j and N_j respectively. For zero applied bias, $P_j = P_m$ and $N_j = N_m$. When a bias is applied, $P_j \neq P_m$ and $N_j \neq N_m$, as is shown dotted in the concentration profile.

and P_j respectively, will increase for a forward bias and decrease for a reverse bias, but will remain unaltered in the fixed charge regions at the solution lattice boundaries. This is shown as the dotted lines for concentration profiles in Fig. 3. The electrostatic potential profile is also shown dotted. The effect of the applied bias on the potential profile is to change the junction potential only, since Ψ_i and Ψ_o are fixed by N^-, N^+, and N_o, P_o, and N_i, P_i, all of which are constant for the system. This is shown in Fig. 4.

P_M and N_M will not be altered by applying a bias, since the change in the ratio of P_M/P_m is taken up by a change in P_m rather than P_M since $P_M \gg P_m$ (see discussion in Appendix A).

Thus, if the minority $+ve$ and $-ve$ mobile ion concentrations at the depletion layer boundary at $x = \pm\lambda$ are P_j and N_j respectively, then;

$$P_j = P_m e^{+qV/KT} \quad \text{and} \quad N_j = N_m e^{+qV/KT} \tag{7}$$

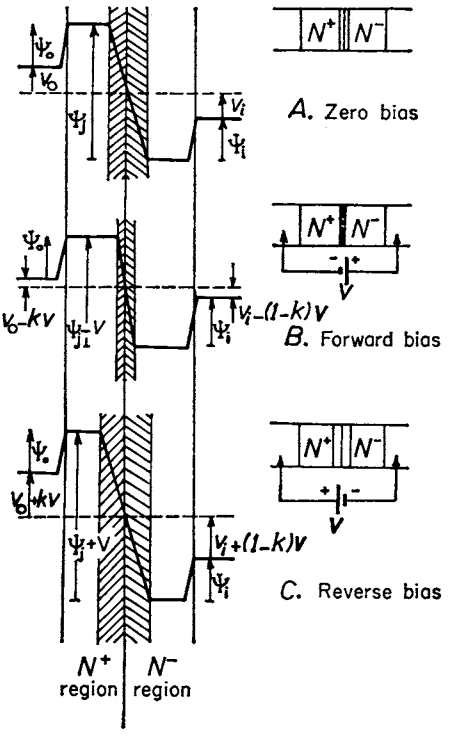

FIGURE 4 Exaggerated and idealized profiles of the electrostatic potential, ψ, for a double fixed charge lattice, with *a* zero applied bias, *b*, forward applied bias, and *c* reverse applied bias. In each case $V_o + V_i$ is the usual membrane potential V_m. V is the applied bias. Note that ψ_o and ψ_i remain constant and hence all the applied bias appears across the junction. The depletion layer in each case is shown shaded.

It can be seen that for a large negative bias, *i.e.*, one that increases the junction potential,

$$P_j \ll P_m \quad \text{and} \quad N_j \ll N_m$$

In order to obtain an expression for the electric current that flows when a bias voltage is applied to the system under consideration, it must be remembered that the applied bias appears almost completely across the junction alone. The mobile ion concentration profile in the depletion layer then shifts in such a way that the mobile ions are again in electrochemical equilibrium. The concentrations of the minority ions at the boundary of the depletion layer, in the N^+ and N^- regions, are then P_j and N_j respectively (equation 7). This sets up a concentration gradient of the minority ions in the fixed charge regions outside the depletion layer. The latter will cause minority ions to diffuse down these concentration gradients. Simultaneously a flow of majority ions of the same sign, from the opposite fixed charge regions, maintains the values of P_j and N_j demanded by the junction potential (see equation 7).

The magnitude of the electric current will hence be determined by the diffusion rate of minority ions through the N^+ and N^- fixed charge regions outside the depletion layer where the concentration of the minority ions now differ from their

former equilibrium values. The diffusion rate is in turn dominated by the concentration gradients. (This point is discussed in more detail in Appendix A.)

Considering for the moment the positive mobile ions only (a similar argument will hold for the negative ions),

$$\frac{d}{dt}[P(x)] + \text{Div. } \Phi(x) = 0 \tag{8}$$

This is just the hydrodynamic equation of continuity, where $\Phi(x)$ is the flux of positive mobile ions at x.

$$\Phi(x) = -D_p \frac{d}{dx}[P(x)], \tag{9}$$

where D_p is the diffusion constant for the positive mobile ions.

It follows from equations (8) and (9) that

$$\frac{d}{dt}[P(x)] - D_p \frac{d^2}{dx^2}[P(x)] = 0 \tag{10}$$

For steady state conditions, that is when the current is constant,

$$\frac{d}{dt}[P(x)] = 0$$

hence it follows from equation (10) that,

$$\frac{d}{dx}[P(x)] = \text{constant} \tag{11}$$

If we denote the width of the N^+ and N^- charge regions outside the depletion layer by W then,

$$W_{N^+} = W_0 - \lambda_{N^+} \tag{12}$$

$$W_{N^-} = W_0 - \lambda_{N^-} \tag{13}$$

where λ_{N^+} and λ_{N^-} are the widths of the depletion layer in the N^+ and N^- lattices.

Using the boundary conditions, $P(x) = P_m$ at $x = -W_o$ and $P(x) = P_j$ at $x = -\lambda$ and using the above definitions of W_{N^+} and W_{N^-}, it follows from equation (11) that;

$$\Phi(x) = \frac{D_p(P_j - P_m)}{W_{N^+}} \tag{14}$$

and hence the electric current density due to the positive mobile ions is given by,

$$J^+(p) = q\Phi(x) = q\frac{D_p(P_j - P_m)}{W_{N^+}} \tag{15}$$

A similar expression holds for the current carried by the negative ions in the N^- region, *i.e.*,

$$J^+(n) = q \frac{D_n}{W_{N^-}} (N_i - N_m) \tag{16}$$

(A flow of positive ions from right to left is taken as a positive current.)

Substituting for P_j and N_j in equations (14) and (15), from equation (7), the current due to the positive ions becomes,

$$J_p^+ = q \frac{D_p}{W_{N^+}} P_m[e^{+qV/KT} - 1] \tag{17}$$

The corresponding current carried by the negative ions is given by

$$J_n^+ = q \frac{D_n}{W_{N^-}} N_m[e^{+qV/KT} - 1] \tag{18}$$

The total current density, J_T is then given by,

$$J_T^+ = J_p^+ + J_n^+ \tag{19}$$

$$= J_G[e^{qV/KT} - 1] \tag{20}$$

where

$$J_G = q\left[\frac{D_p P_m}{W_{N^+}} + \frac{D_n N_m}{W_{N^-}}\right]$$

It can be seen from equation (20) that this system displays the property of rectification since, for a forward bias, *i.e.*, V positive, the current J_T^+ increases. For large values of V (*i.e.*, such that $qV \gg KT$) the forward current is given by,

$$J_T^+ = J_G e^{qV/KT}, \qquad qV \gg KT \tag{21}$$

For a reverse bias *i.e.*, V negative, the current rapidly decreases and becomes almost independent of V for $qV \ll KT$

$$i.e. \qquad J_T^- \text{ (reverse)} = J_G, \qquad qV \ll KT$$

For small values of V, such that $qV \approx KT$, the junction behaves substantially as an ohmic resistance, rectification not becoming predominant until larger values of $|qV|$ are involved.

The Punch-Through Effect. It can be shown (see Appendix B) that W_{N^+} and W_{N^-} decrease with applied reverse bias so that this will tend to increase the reverse current and in the limit when W_{N^+} or $W_{N^-} \to 0$ the current will increase out of control, which is the breakdown point of such a system.

For simplicity it will be now assumed that N^+ and N^- are such that $\lambda_{N^+} = \lambda_{N^-} = \lambda$. This point is discussed in more detail in Appendix B.

If $\lambda_{N^+} = \lambda_{N^-} = \lambda$, then it follows that $W_{N^+} = W_{N^-} = W$ and hence

$$W = W_0 - \lambda$$

An expression for λ can be obtained by solving Poisson's equation in the depletion layer (see Appendix B). This yields,

$$W = W_0 - \left[\frac{\epsilon(\Psi_j - V)}{q(N^- + N^+)/2}\right]^{1/2} \tag{22}$$

Hence from equation (20) the current density becomes,

$$J_T^+ = \frac{1}{W_0 - \left[\frac{\epsilon(\Psi_j - V)}{q(N^- + N^+)/2}\right]^{1/2}} J_G'[e^{qV/KT} - 1] \tag{23}$$

Where J_G' is defined by, $J_G' = q\,(D_p P_m + D_n N_m)$.

For a forward bias $(\Psi_j - V)$ is small and hence λ is small and hence $W = W_o - \lambda \approx W_o$ and the current essentially increases by the factor

$$[e^{qV/KT} - 1]^{qV/KT} \quad \text{if} \quad qV \gg KT$$

For the case of reverse bias (*i.e.*, V negative), the current will at first decrease with V and when $-qV$ becomes greater than KT the reverse current will become almost independent of V, as before, if W remained constant. As shown in equation (22), however, W will decrease with increasing reverse bias and hence it follows from equation (23) that J_T^- (reverse) will increase. The exponential factor $e^{qV/KT}$ however will swamp the $1/(V)^{\frac{1}{2}}$ factor for moderate values of V. When $\lambda \to W_o$ however, $W \to 0$ and the reverse current will then increase very rapidly. In the limit when $\lambda = W_o$, the depletion layer boundary will be at the lattice solution boundary and the reverse current will then increase uncontrollably.

The increase in current at moderate values of V may be termed the "early" effect. The sudden rapid increase in current, when V (reverse) is so large that $\lambda \to W_o$ and $W \to 0$, may be termed the "punch-through" effect.

It can be shown (see Appendix B) that Ψ_j, the junction potential, is given by,

$$\Psi_j = \frac{KT}{q} \ln \frac{N^+ N^-}{P_i N_0} + V_m \tag{24}$$

and hence from equation (22) by substituting for $\Psi_j - V$ from equation (24),

$$W = W_0 - \left[\frac{\epsilon\left[(V_m - V) + \frac{KT}{q} \ln \frac{N^- N^+}{P_i N_0}\right]}{q(N^- + N^+)/2}\right]^{1/2}$$

Thus "punch-through" should occur when

$$W_0 = \left[\frac{\epsilon\left[(V - V) + \frac{KT}{q} \ln \frac{N^- N^+}{P_i N_0}\right]}{q(N^- + N^+)/2}\right]^{1/2}$$

If ε and N^- and N^+ for the membrane were known and since P_i and N_o are known, it should be possible to predict at what total membrane potential difference, $V_m - V$, "punch-through" is going to occur, for a given membrane thickness, $2W_o$.

Conversely, from the observed value of $V_m - V$ at which breakdown occurs it should be possible to estimate a combination of ε, N, and $2W_o$ for the membrane.

EXPERIMENTAL METHODS

The materials used in the experiments were members of the Characeae, *Chara australis* and *Nitella* sp. The unusual large dimensions of these cells enables the manipulation of electrodes and material to be carried out with ease.

The cells selected for the experiments were usually whorl cells, 10 to 15 mm long and 1 to 1.5 mm in diameter for *Chara australis* and approximately 0.5 mm in diameter for *Nitella* sp.

Cells used were separated from a filament of cells and mounted on a Perspex mount, and were irrigated during the course of the experiment with a flowing solution containing 1.0 mN NaCl and 0.1 mN KCl.

Two glass microelectrodes filled with 3N KCl were inserted into the cell, using micromanipulators. One of the electrodes was used to pass current through the cell membranes, a silver chloride coated silver wire grid in the external solution being used as the other electrode.

The second electrode inserted into the cell was used to measure the membrane potential difference, using an external KCl-in-agar filled electrode just outside the cell as a reference. Separate experiments were done with the potential measuring microelectrode in the vacuole and in the cytoplasm. Both the current passed and the membrane potential difference were recorded on a twin channel chart recorder.

The current passed through the membrane was scanned using a linearly increasing (or decreasing) current supplied by a Miller sweep circuit. A resistance of 10^7 ohms in series with the sweep generator insured that the current passed is controlled by the output voltage of the sweep generator and is not affected by changes in membrane resistance.

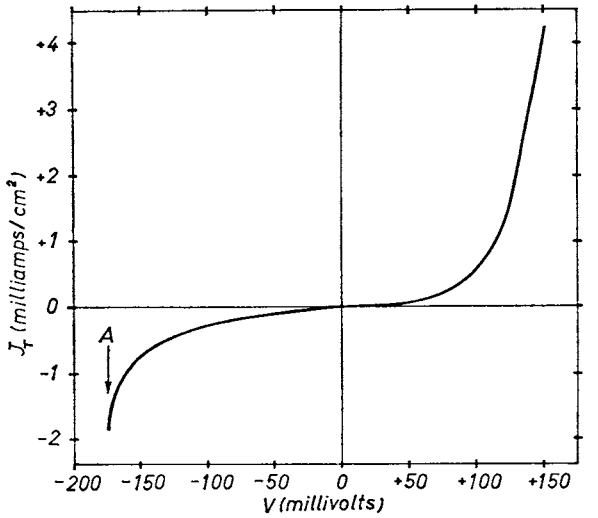

FIGURE 5 A plot of equation (23). The thickness of the depletion layer, 2λ, was calculated using the parameters used to calculate W_o (see Discussion). J'_o was chosen to fit the experimentally observed V-I characteristics; T was taken as 293K. At "A" "punch-through" occurs.

RESULTS

Fig. 6 is a reproduction of the V-I characteristics of the plasmalemma and tonoplast in series (*i.e.*, vacuolar microelectrode) of *Chara australis*, taken from the chart recorder. Fig. 7 is a reproduction of the V-I characteristics of the plasmalemma alone (*i.e.*, cytoplasmic microelectrode). Fig. 8 is the corresponding V-I characteristic of the plasmalemma and tonoplast in series of *Nitella* sp.

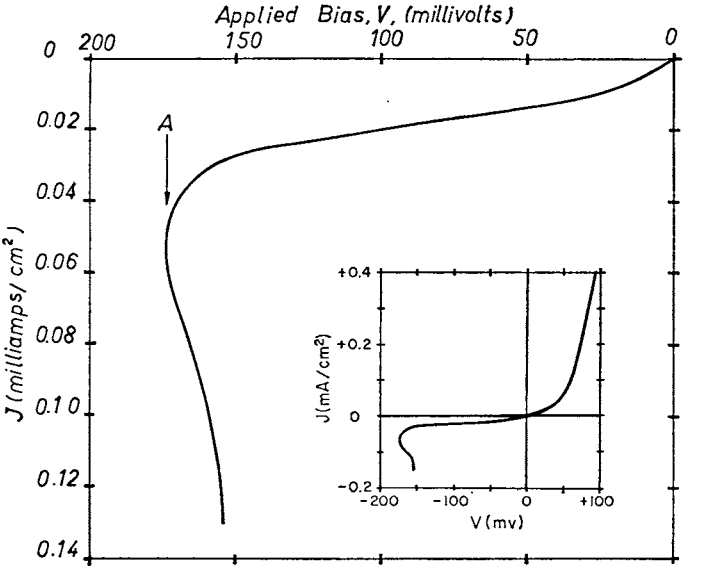

FIGURE 6 A record of the V-I characteristics, taken from the chart recorder, for the plasmalemma and tonoplast in series (*i.e.*, vacuolar microelectrode) of *Chara australis*. A point "A" "punch-through" has occurred. V_m for this cell was approximately 125 mv (*i.e.*, $V_m - V \approx 300$ mv).

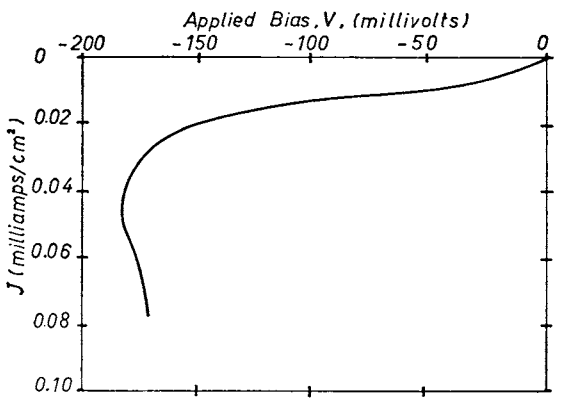

FIGURE 7 A record of the V-I characteristics, taken from the chart recorder, for the plasmalemma of *Chara australis*. The resting potential difference across the plasmalemma was approximately 120 mv, hence $V_m - V \approx 300$ mv.

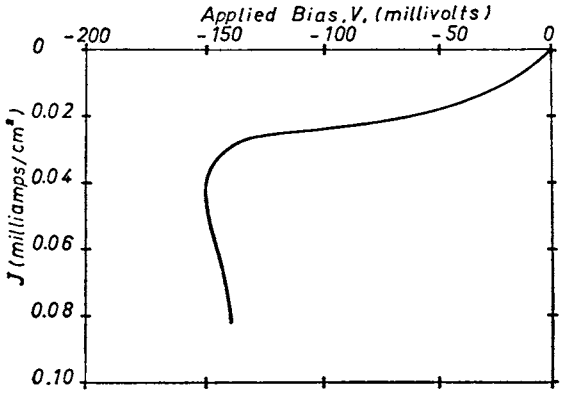

FIGURE 8 A record of the V-I characteristics, for the plasmalemma and tonoplast in series of *Nitella* sp. "Punch-through" occurs at approximately at $V = -150$ mv. V_m for this cell was 150 mv, hence $V_m - V \approx 300$ mv.

The scans cannot normally be done in the depolarizing direction (*i.e.*, V positive) beyond about +50 mv applied potential bias. This is because these cells will give action potentials when the membrane is depolarized by more than about 50 mv (Findlay 1962, Hope 1961, Findlay and Hope 1964).

To overcome this difficulty for depolarizing currents, the cells were sometimes soaked for about 10 minutes in a solution of 1 mN $MgCl_2$. This lowers the concentration of Ca^{++} ions in the cell wall by exchange with Mg^{++}. Under these conditions action potentials cannot be initiated (Hope, 1961).

Whether the cells are soaked in $MgCl_2$ or not, the curves for hyperpolarizing currents (*i.e.*, applied V negative) are of the same form and in every case the breakdown effect can be observed. The breakdown effect occurs approximately at 300 mv, that is at $V_m - V \approx 300$ mv.

DISCUSSION

It can be seen from Figs. 6, 7, and 8 that near the "punch-through"' point the slope of the V-I characteristics becomes very steep. Beyond "punch-through" a large change in current produces virtually no change in potential. Comparison of Fig. 6 and Fig. 7 shows that the V-I characteristic of the plasmalemma alone is substantially the same as that of the two membranes (*i.e.*, plasmalemma and tonoplast) in series. This is to be expected as the resistance of the plasmalemma is about ten times that of the tonoplast (Findlay and Hope, 1964). Comparison of Fig. 6 and Fig. 8 shows that the V-I characteristics, including "punch-through," of the membranes of *Nitella* sp. are very similar to those of *Chara australis*. By comparison of Fig. 5 with the inset on Fig. 6 it can be seen that the predicted and experimental V-I characteristics are very similar for regions removed from the "punch-through" point.

The experimental curves show that the reverse current increases with increasing reverse bias (*i.e.*, V more negative). It is interesting to note that the plot of equation (23) (see Fig. 5) also shows this increase in J^- (reverse) with decreasing V (due to $W = W_o - \lambda$ decreasing, as discussed previously).

The fact that the slope of the V-I characteristics near the "punch-through" point as predicted by equation (23) is not the same as that found experimentally, is probably due to an omission of energy terms, such as the particle-particle interaction energy in the Maxwell-Boltzmann distribution law, and the assumption that the profiles for ψ and mobile ion concentration near the solution lattice boundary rise in the lattice to their maximum value in a negligible distance.

If we assume an average fixed charge concentration of 0.1 normal (*i.e.*, 6×10^{25} charges/m^3), a quite probable value, and if we assume that $\varepsilon_R = 30$ (ε_R for water $= 80$ and ε_R for olive oil $= 3$), then using the experimentally observed value for $(V_m - V)$ at which "punch-through" occurs, we can estimate a value of $2W_o$.

Thus, at "punch-through,"

$$2W_0 = \left[\frac{4\epsilon\left[(V_m - V) + \frac{KT}{q}\ln\frac{N^-N^+}{P_i N_0}\right]}{q(N^- + N^+)/2}\right]^{1/2}$$

where $\varepsilon = \varepsilon_R\varepsilon_o$, $q = |e| = 1.6 \times 10^{-19}$ coul.

P_i in the cytoplasm of these cells is not accurately known. However MacRobbie (1962) has developed a technique to analyze the concentration of cations in the cytoplasm and found that the sum of (K^+) and (Na^+) was in the range of 100 to 150 mN. The external solution contained 1.0 mN NaCl and 0.1 mN KCl (*i.e.*, $P_0 = N_o = 1.1$ mN).

Using the experimental value of +300 mv for $(V_m - V)$ at "punch-through";

$$2W_0 = 6.8 \times 10^{-9} \text{ m}$$

$$\approx 70\ A$$

This value is certainly not an unreasonable value since the membrane thickness has been estimated by various workers to be approximately 75 A (Briggs, Hope, and Robertson, 1961).

Further experiments on the "punch-through" effect as a function of the external concentration of various ions, as well as isotope tracer experiments to determine the identity of the punching ion or ions are still being undertaken. It is hoped to publish the results of the experiments at a later date.

It may be pointed out that this derived value for $2W_o$ may be quite erroneous, since it depends on our choice of ε and N^- and N^+. However, the fact that the order of magnitude is consistent with other estimates when not unreasonable values of N and ε are assumed in the calculations, seems significant.

It may be emphasized that the model used in this paper is a rather idealized one.

In actual biological membranes, the $N+ - N-$, junction need not necessarily be an "abrupt" one, $\lambda_{N^+} \neq \lambda_{N^-}$, and the charge distribution may be such that the lattice displays selective ionic absorption (see below). These things would complicate the mathematical analysis of the system. However, the V-I characteristics of such a system would be similar, even if not as striking, as that of our idealized system.

A double lattice fixed charge membrane can be successfully applied to deal with rectification and the observed punch-through effect. This together with the fact that fixed charge membrane models can also deal with capacitance (Mauro, 1962) and, as Eisenman (1960) has shown, equilibrium ionic specificity and cellular potentials seems to indicate that this type of model has much to commend it.

It should be pointed out however that the model as presented in this paper, cannot, when considered as a Donnan system, explain the sign of the observed membrane potential.

APPENDIX A

When a bias is applied it appears across the depletion layer. This causes an imbalance in the mobile ion concentrations. Thus for the positive mobile ions the new concentrations will be related to the zero bias ones by the relation

$$\frac{P_m^*}{P_M^*} = \frac{P_m e^{qV/KT}}{P_M}$$

where P_m^* and P_M^* are the new minority and majority positive mobile ion concentrations respectively.

To satisfy this equation for a forward bias either P_m^* must increase or P_M^* decrease.

However, since $P_m \ll P_M$ the increase in the ratio of P_m^*/P_M^* when a forward bias is applied will be taken up by P_m^*, as a decrease of P_M^* in the same ratio would imply an impossibly large space charge imbalance outside the depletion layer in the fixed charge lattice.

A similar argument applies for the case of a reverse bias.

Hence it can be assumed that it is the minority ion concentration, P_m, that will increase to P_j at the depletion layer boundary in the N^+ region when a forward bias is applied, P_j being related to P_m by

$$P_j = P_m e^{qV/KT}$$

This increase in the concentration of the minority positive mobile ion concentration at the depletion layer boundary will tend to establish an electric field in the N_+ region between the depletion layer boundary and the solution lattice interface. This field in turn will tend to increase the concentration of majority negative mobile ions at the depletion layer boundary in the N^+ region. This in turn will reduce the space charge and hence the electric field itself. The concentration of these negative mobile ions will increase until the concentration gradient so established is such that their tendency to diffuse back is just balanced by the weak electric field. At this stage there is no net movement

of negative majority mobile ions in the N^+ region. The electric current in the N^+ region is hence just due to the diffusion of minority positive mobile ions.

A similar argument shows that the current in the N^- fixed charge region is just due to the diffusion of minority negative mobile ions.

The diffusion of the minority mobile ions is dominated by the hydrodynamic diffusion. This can be seen from,

$$J(+ve \text{ ions}) = -qD_p \frac{dP(x)}{dx} + qP(x)\mu_p E(x)$$

where μ_p is the mobility, and $P(x)$ the concentration of the positive mobile ions $(P_j > P(x) > P_m)$. $E(x)$ is the electric field at x.

Now since both $E(x)$ and $P(x)$ are small compared to $[d\,P(x)/dx]$ it can be seen that the current is dominated by hydrodynamic diffusion.

APPENDIX B

Since $W_\bullet$ is fixed by the geometrical dimensions of the membrane and since;

$$\begin{aligned} W_{N^+} &= W - \lambda_{N^+} \\ W_{N^-} &= W_0 - \lambda_{N^-} \end{aligned} \tag{1'}$$

it is necessary to find the dependence of λ_{N^+} and λ_{N^-} on the applied bias V, in order to see how this affects W_{N^+} and W_{N^-}.

The width of the depletion layer can be determined as follows. From Poisson's equation the electric potential, ψ, in the depletion region is given by,

$$\frac{d^2\psi}{dx^2} = -\frac{\rho}{\epsilon} \tag{2'}$$

Using the idealized space charge distribution depicted in Fig. 3 and since the space change is almost solely due to the uncompensated fixed charges in the depletion layer,

$$\frac{d^2\psi}{dx^2} = \frac{qN^-}{\epsilon} \quad \text{for} \quad x > 0$$

and (3')

$$\frac{d^2\psi}{dx^2} = \frac{-qN^+}{\epsilon} \quad \text{for} \quad x < 0$$

On integration, these equations yield,

$$\psi(x = \lambda_{N^-}) = \frac{qN^-}{2\epsilon}\lambda_{N^-}{}^2$$

and (4')

$$\psi(x = \lambda_{N^+}) = \frac{qN^+}{2\epsilon}\lambda_{N^+}{}^2$$

But $$\psi(x = \lambda_{N^-}) = \psi_i + V_i$$

and $$\psi(x = \lambda_{N^+}) = \psi_0 + V_0$$

hence
$$\psi_i + V_i = \frac{qN^-}{2\epsilon}\lambda_{N^-}{}^2$$

and
$$\psi_0 + V_0 = \frac{qN^+}{2\epsilon}\lambda_{N^+}{}^2 \tag{5'}$$

In general, for an asymmetric model, *i.e.*, one in which $N^+ \neq N^-$ and/or the internal and external ionic solutions are not of equal concentration, $\lambda_{N^-} \neq \lambda_{N^+}$. In this case electrical breakdown will occur when either λ_{N^-} or λ_{N^+} equals W_o, that is when either W_{N^-} or $W_{N^+} \to o$. The mathematical treatment of this case is rather cumbersome, hence for simplicity it will be assumed that for the given external and internal ionic solution concentration, N^- and N^+ are such that,

$$\lambda_{N^-} = \lambda_{N^+}$$

Now since $P_i\ (= N_i) \neq P_o\ (= N_o)$ in our case, this implies that $N^- \neq N^+$.

So assuming that $\lambda_{N^-} = \lambda_{N^+} = \lambda$, and hence $W_{N^-} = W_{N^+} = W$, then from equation (5') and from the fact that,

$$\psi_i = \psi_i + V_i + \psi_0 + V_0,$$
$$\psi_i = \frac{q}{\epsilon}\lambda^2\left[\frac{N^- + N^+}{2}\right]$$

Hence the total width of the depletion layer, 2λ, is given by,

$$2\lambda = \left[\frac{4\psi_i\epsilon}{q(N^- + N^+)/2}\right]^{1/2} \tag{6'}$$

If the junction is biased then as pointed out before the biasing voltage appears almost completely across the junction.

In this case,

and
$$\psi(x = \lambda_{N^-}) = \psi_i + V_i + (1 - k)V$$
$$\psi(x = \lambda_{N^+}) = \psi_0 + V_0 + kV \tag{7'}$$

where k is the fraction of the biasing voltage that appears across the N^+ half of the junction.

In this case,

$$\psi_i - V = \psi_i + V_i + \psi_0 + V_0 \tag{8'}$$

and hence equation (6') then becomes

$$2\lambda = \left[\frac{4\epsilon(\psi_i - V)}{q(N^- + N^+)/2}\right]^{1/2} \tag{9'}$$

It can thus be seen that the width of the depletion layer will decrease with increasing forward bias and increase with increasing reverse bias (*i.e.*, V negative).

The width of the fixed charge regions outside the depletion layer, for each of the N^+ and N^- regions can then be obtained from,

$$W = W_0 - \lambda$$

and hence

$$W = W_0 - \left[\frac{\epsilon(\psi_i - V)}{q(N^- + N^+)/2}\right]^{1/2} \tag{10'}$$

In order to obtain an expression for Ψ_j, the junction potential, it is necessary to solve equation 4;
viz,

$$\frac{d^2\Psi(x)}{dx^2} = \frac{2qN_0}{\epsilon}\left[\sinh\frac{q\Psi(x)}{KT} - \frac{N^+}{2N_0}\right]$$

where $N_o = P_o$, is the concentration of mobile ions in the solution phase at large distances from the lattice boundary.

For large distances from the boundary inside the lattice, $[d\Psi(x)/dx]$ and $[d^2\Psi(x)/dx^2]$ $\rightarrow 0$ as $x \rightarrow +\infty$. Hence from equation (4),

$$\sinh\frac{q\Psi(+\infty)}{KT} = \frac{N^+}{2N_0} \tag{11'}$$

and since

$$\sinh\frac{q\Psi(x)}{KT} = \tfrac{1}{2}[e^{+q\Psi(x)/KT} - e^{-q\Psi(x)/KT}] \tag{12'}$$

and also since for $N^+ \gg N_o$, the second term in the bracket of equation (12'), is small compared to the first term, it follows that;

$$\tfrac{1}{2}e^{+q\psi(+\infty)/KT} \approx \frac{N^+}{2N_0}$$

$$i.e., \qquad \psi(+\infty) = \frac{KT}{q}\ln\frac{N^+}{N_0} \tag{13'}$$

But $\Psi_{+\infty}$ is the limiting value of the electrostatic potential in the lattice, which was indicated as Ψ_o for the left-hand side, and as Ψ_i for the right-hand side. Mauro (1962) has shown that the electrostatic potential in the lattice rises very rapidly, and hence rapidly reaches its limiting value. Thus for the left-hand side solution lattice interface,

$$\psi_0 = \frac{KT}{q}\ln\frac{N^+}{N_0} \tag{14'}$$

and for the right-hand side,

$$\psi_i = \frac{KT}{q}\ln\frac{N^-}{P_i} \tag{15'}$$

Thus

$$\psi_i + \psi_0 = \frac{KT}{q}\ln\frac{N^-N^+}{P_iN_0} \tag{16'}$$

From Fig. 3 it can be seen that,

$$\Psi_j = \Psi_i + \Psi_0 + V_m \tag{17'}$$

where V_m is the membrane potential, $V_m = V_i + V_o$.

Thus from equations (16′) and (17′),

$$\Psi_i = \frac{KT}{q} \ln \frac{N^+ N^-}{P_i N_0} + V_m \qquad (18')$$

The author wishes to thank Mr. P. H. Barry for his helpful discussions on this work.

Received for publication, December 28, 1964.

REFERENCES

BRIGGS, G. E., HOPE, A. B., and ROBERTSON, R. N. 1961, Electrolytes and Plant Cells, Oxford, England, Blackwell Scientific Publications.

EISENMAN, G., 1960, On the elementary atomic origin of equilibrium ionic specificity. Symposium on membrane transport and metabolism, New York, Academic Press, 163.

FINDLAY, G. P., 1962, Calcium ions and the action potential in *Nitella, Australian J. Biol. Sc.*, **15**, 69.

FINDLAY, G. P., and HOPE, A. B., 1964, Ionic Relations of cells of *Chara australis* VII, The separate electrical characteristics of the plasmalemma and the tonoplast, *Australian J. Biol. Sc.*, **17**, 62.

HOPE, A. B., 1961, Ionic relations of cells of *Chara australis* V, The action potential, *Australian J. Biol. Sc.*, **14**, 312.

GOLDMAN, D. E., 1943, Potential impedance and rectification in membranes, *J. Gen. Physiol.*, **27**, 37.

KITTEL, C., 1957, Introduction to solid state physics, New York, John Wiley & Sons Inc.

LE CAN, C., HART, K., and DE RUYTER, C., 1962, The Junction Transistor as a switching device, Eindhoven, The Netherlands, Philips Technical Library.

MAURO, A., 1962, Space charge regions in fixed charge membranes and the associated property of capacitance, *Biophysic. J.*, **2**, 179.

MACROBBIE, E. A. C., 1962, Ionic relations of *Nitella translucens, J. Gen. Physiol.* **45**, 86.

TEORELL, T., 1953, Transport processes and electrical phenomena in ionic membranes, *Progr. Biophysics and Biophysic. Chem.*, **3**, 30.